

# **TITLE PAGE**

2

## **TITLE:**

**Predicting and elucidating the etiology of fatty liver disease using a machine learning-based approach: an IMI DIRECT study**

6

## **AUTHORS:**

Naeimeh Atabaki-Pasdar<sup>1</sup>, Mattias Ohlsson<sup>2,3</sup>, Ana Viñuela<sup>4,5,6</sup>, Francesca Frau<sup>7</sup>, Hugo Pomares-Millan<sup>1</sup>, Mark Haid<sup>8</sup>, Angus G Jones<sup>9</sup>, E Louise Thomas<sup>10</sup>, Robert W Koivula<sup>1,11</sup>, Azra Kurbasic<sup>1</sup>, Pascal M Mutie<sup>1</sup>, Hugo Fitipaldi<sup>1</sup>, Juan Fernandez<sup>1</sup>, Adem Y Dawed<sup>12</sup>, Giuseppe N Giordano<sup>1</sup>, Ian M Forgie<sup>12</sup>, Timothy J McDonald<sup>9,13</sup>, Femke Rutters<sup>14</sup>, Henna Cederberg<sup>15</sup>, Elizaveta Chabanova<sup>16</sup>, Matilda Dale<sup>17</sup>, Federico De Masi<sup>18</sup>, Cecilia Engel Thomas<sup>17</sup>, Kristine H Allin<sup>19,20</sup>, Tue H Hansen<sup>19,21</sup>, Alison Heggie<sup>22</sup>, Mun-Gwan Hong<sup>17</sup>, Petra JM Elders<sup>23</sup>, Gwen Kennedy<sup>24</sup>, Tarja Kokkola<sup>25</sup>, Helle Krogh Pedersen<sup>19</sup>, Anubha Mahajan<sup>26</sup>, Donna McEvoy<sup>22</sup>, Francois Pattou<sup>27</sup>, Violeta Raverdy<sup>27</sup>, Ragna S Häussler<sup>17</sup>, Sapna Sharma<sup>28,29</sup>, Henrik S Thomsen<sup>16</sup>, Jagadish Vangipurapu<sup>25</sup>, Henrik Vestergaard<sup>19,30</sup>, Leen M 't Hart<sup>14,31,32</sup>, Jerzy Adamski<sup>8,33,34</sup>, Petra B Musholt<sup>35</sup>, Soren Brage<sup>36</sup>, Søren Brunak<sup>18,37</sup>, Emmanouil Dermitzakis<sup>4,5,6</sup>, Gary Frost<sup>38</sup>, Torben Hansen<sup>19,39</sup>, Markku Laakso<sup>25,40</sup>, Oluf Pedersen<sup>19</sup>, Martin Ridderstråle<sup>41</sup>, Hartmut Ruetten<sup>7</sup>, Andrew T Hattersley<sup>9</sup>, Mark Walker<sup>22</sup>, Joline WJ Beulens<sup>14,42</sup>, Andrea Mari<sup>43</sup>, Jochen M Schwenk<sup>17</sup>, Ramneek Gupta<sup>18</sup>, Mark I McCarthy<sup>11,26,44,45</sup>, Ewan R Pearson<sup>12</sup>, Jimmy D Bell<sup>10</sup>, Imre Pavo<sup>46</sup>, Paul W Franks<sup>1,47,48</sup>.

22

## **AFFILIATIONS:**

24

<sup>1</sup> Genetic and Molecular Epidemiology Unit, Department of Clinical Sciences, Lund University, Malmö, Sweden.

<sup>2</sup>Department of Astronomy and Theoretical Physics, Computational Biology and Biological Physics

**NOTE: This preprint reports new research that has not been certified by peer review and should not be used to guide clinical practice.**  
Unit, Lund University, Sweden.

- 29 <sup>3</sup> Center for Applied Intelligent Systems Research, Halmstad University, Sweden.
- 30 <sup>4</sup> Department of Genetic Medicine and Development, University of Geneva Medical School, CH-
- 31 1211 Geneva, Switzerland.
- 32 <sup>5</sup> Institute for Genetics and Genomics in Geneva (iGE3), University of Geneva Medical School, CH-
- 33 1211 Geneva, Switzerland.
- 34 <sup>6</sup> Swiss Institute of Bioinformatics, CH-1211 Geneva, Switzerland.
- 35 <sup>7</sup> Sanofi-Aventis Deutschland GmbH, Frankfurt am Main, Germany.
- 36 <sup>8</sup> Research Unit Molecular Endocrinology and Metabolism, Helmholtz Zentrum München, German
- 37 Research Center for Environmental Health, Neuherberg, Germany.
- 38 <sup>9</sup> The Institute of Clinical and Biological Sciences, University of Exeter College of Medicine and
- 39 Health, University of Exeter, Exeter, UK.
- 40 <sup>10</sup> Research Centre for Optimal Health, School of Life Sciences, University of Westminster, London,
- 41 UK.
- 42 <sup>11</sup> Oxford Centre for Diabetes, Endocrinology and Metabolism, Radcliffe Department of Medicine,
- 43 University of Oxford, Oxford, UK.
- 44 <sup>12</sup> Population Health & Genomics, School of Medicine, University of Dundee, Ninewells Hospital,
- 45 Dundee, UK.
- 46 <sup>13</sup> Blood Sciences, Royal Devon and Exeter NHS Foundation Trust, Exeter, UK.
- 47 <sup>14</sup> Amsterdam UMC, location VUmc, Department of Epidemiology and Biostatistics, Amsterdam
- 48 Public Health research institute, Amsterdam, the Netherlands.
- 49 <sup>15</sup> Department of Endocrinology, Abdominal Centre, Helsinki University Hospital, Helsinki,
- 50 Finland.
- 51 <sup>16</sup> Department of Diagnostic Radiology, Copenhagen University Hospital Herlev Gentofte, Herlev,
- 52 Denmark.
- 53 <sup>17</sup> Affinity Proteomics, Science for Life Laboratory, School of Engineering Sciences in Chemistry,
- 54 Biotechnology and Health, KTH - Royal Institute of Technology, Solna, Sweden.
- 55 <sup>18</sup> Department of Health Technology, Technical University of Denmark, Kongens Lyngby,
- 56 Denmark.

- 57 <sup>19</sup> Novo Nordisk Foundation Center for Basic Metabolic Research, Faculty of Health and Medical  
58 Sciences, University of Copenhagen, Copenhagen, Denmark.
- 59 <sup>20</sup> Center for Clinical Research and Prevention, Bispebjerg and Frederiksberg Hospital, The Capital  
60 Region, Copenhagen, Denmark.
- 61 <sup>21</sup> Department of Cardiology and Endocrinology, Slagelse Hospital, Slagelse, Denmark.
- 62 <sup>22</sup> Institute of Cellular Medicine (Diabetes), Newcastle University, Newcastle upon Tyne, UK.
- 63 <sup>23</sup> Department of General Practice, Amsterdam UMC – location VUmc, Amsterdam Public Health  
64 research institute, Amsterdam, The Netherlands.
- 65 <sup>24</sup> The Immunoassay Biomarker Core Laboratory, School of Medicine, University of Dundee,  
66 Ninewells Hospital, Dundee, UK.
- 67 <sup>25</sup> Institute of Clinical Medicine, Internal Medicine, University of Eastern Finland, Kuopio, Finland.
- 68 <sup>26</sup> Wellcome Centre for Human Genetics, University of Oxford, Oxford, UK.
- 69 <sup>27</sup> University of Lille, Inserm, UMR 1190, Translational Research in Diabetes, CHU Lille Endocrine  
70 Surgery, 59000 Lille, France.
- 71 <sup>28</sup> German Center for Diabetes Research, Neuherberg, Germany.
- 72 <sup>29</sup> Unit of Molecular Epidemiology, Institute of Epidemiology II, Helmholtz Zentrum München,  
73 Germany.
- 74 <sup>30</sup> Steno Diabetes Center Copenhagen, Gentofte, Denmark.
- 75 <sup>31</sup> Department of Cell and Chemical Biology, Leiden University Medical Center, the Netherlands.
- 76 <sup>32</sup> Department of Biomedical Data Sciences, Section Molecular Epidemiology, Leiden University  
77 Medical Center, the Netherlands.
- 78 <sup>33</sup> Lehrstuhl für Experimentelle Genetik, Technische Universität München, Freising-  
79 Weihenstephan, Germany.
- 80 <sup>34</sup> Department of Biochemistry, Yong Loo Lin School of Medicine, National University of  
81 Singapore, Singapore.
- 82 <sup>35</sup> Sanofi, Diabetes Division, Research and Development, Frankfurt, Germany.
- 83 <sup>36</sup> MRC Epidemiology Unit, University of Cambridge, UK.
- 84 <sup>37</sup> Novo Nordisk Foundation Center for Protein Research, Faculty of Health and Medical Sciences,  
85 University of Copenhagen, Copenhagen, Denmark.

<sup>38</sup> Section for Nutrition Research, Department of Metabolism, Digestion and Reproduction, Imperial College Hammersmith Campus, DuCane Road, London W12 ONN.

<sup>39</sup> Faculty of Health Sciences, University of Southern Denmark, Odense, Denmark.

<sup>40</sup> Department of Medicine, University of Eastern Finland and Kuopio University Hospital, Kuopio, Finland.

<sup>41</sup> Clinical Pharmacology and Translational Medicine, Novo Nordisk A/S, Søborg, Denmark.

<sup>42</sup> Julius Center for Health Sciences and Primary Care, University Medical Center Utrecht, Utrecht, The Netherlands.

<sup>43</sup> Institute of Neuroscience, National Research Council, Padua, Italy.

<sup>44</sup> Oxford NIHR Biomedical Research Centre, Oxford University Hospitals NHS Foundation Trust, John Radcliffe Hospital, Oxford, UK.

<sup>45</sup> OMNI Human Genetics, Genentech, 340 Point San Bruno Blvd, South San Francisco, CA 94080.

<sup>46</sup> Eli Lilly Regional Operations GmbH, Vienna, Austria.

<sup>47</sup> Department of Nutrition, Harvard School of Public Health, Boston, MA, USA.

<sup>48</sup> Department of Public Health & Clinical Medicine, Section for Medicine, Umeå University, Umeå, Sweden.

## **CORRESPONDING AUTHOR:**

Name: Paul W. Franks

Address: Department of Clinical Sciences, Genetic and Molecular Epidemiology Unit, CRC, Building 91, Level 10, Jan Waldenströms gata 35, Skåne University Hospital Malmö, Lund University, SE-205 02, Malmö, Sweden

Tel: +4640391149; Fax: +4640391222;

E-mail: Paul.Franks@med.lu.se

# **ABSTRACT**

**Background:** Non-alcoholic fatty liver disease (NAFLD) is highly prevalent and causes serious health complications in type 2 diabetes (T2D) and beyond. Early diagnosis of NAFLD is important, as this can help prevent irreversible damage to the liver and ultimately hepatocellular carcinomas.

**Methods and Findings:** Utilizing the baseline data from the IMI DIRECT participants (n=1514) we sought to expand etiological understanding and develop a diagnostic tool for NAFLD using machine learning. Multi-omic (genetic, transcriptomic, proteomic, and metabolomic) and clinical (liver enzymes and other serological biomarkers, anthropometry, and measures of beta-cell function, insulin sensitivity, and lifestyle) data comprised the key input variables. The models were trained on MRI image-derived liver fat content (<5% or ≥5%). We applied LASSO (least absolute shrinkage and selection operator) to select features from the different layers of omics data and Random Forest analysis to develop the models. The prediction models included clinical and omics variables separately or in combination. A model including all omics and clinical variables yielded a cross-validated receiver operator characteristic area under the curve (ROCAUC) of 0.84 (95% confidence interval (CI)=0.82, 0.86), which compared with a ROCAUC of 0.82 (95% CI=0.81, 0.83) for a model including nine clinically-accessible variables. The IMI DIRECT prediction models out-performed existing non-invasive NAFLD prediction tools.

**Conclusions:** We have developed clinically useful liver fat prediction models (see: [www.predictliverfat.org](http://www.predictliverfat.org)) and identified biological features that appear to affect liver fat accumulation.

## INTRODUCTION

Non-alcoholic fatty liver disease (NAFLD) is characterized by the accumulation of fat in hepatocytes in the absence of excessive alcohol consumption. NAFLD is a spectrum of liver diseases with its first stage, known as ‘simple steatosis’, defined as liver fat content >5% of total liver weight. Simple steatosis can progress to non-alcoholic steatohepatitis (NASH), fibrosis, cirrhosis, and eventually hepatocellular carcinoma. In NAFLD, triglycerides accumulate in hepatocytes and liver insulin sensitivity is diminished, promoting hepatic gluconeogenesis, thereby raising the risk of type 2 diabetes (T2D) or exacerbating the disease pathology in those with diabetes (1-5).

The prevalence of NAFLD is thought to be around 20-40% in the general population in Western countries, with an increasing trend across the world, imposing a substantial economic and public health burden (6-9). However, the exact prevalence of NAFLD has not been clarified, in part because liver fat is difficult to accurately assess. Liver biopsy, magnetic resonance imaging (MRI), ultrasounds and liver enzyme tests are often used for NAFLD diagnosis, but the invasive nature of biopsies, the high costs of MRI scans, the non-quantitative nature and low sensitivity of conventional ultrasounds, and the low accuracy of liver enzyme tests are significant limitations (10-12). To address this gap, several liver fat prediction indices have been developed, but none of these has sufficiently high predictive ability to be considered a gold standard (10).

The purpose of this study was to use machine learning to identify novel molecular features associated with NAFLD and combine these with conventional clinical variables to predict NAFLD. These models include those variables that are likely to be informative of disease etiology, some of which may be of use in clinical practice.

## **METHODS AND MATERIALS**

### *Participants (IMI DIRECT)*

The primary data utilized in this study were generated within the IMI DIRECT consortium, which includes a multicenter prospective cohort study of 3029 adults recently diagnosed with T2D (n=795) or at high risk of developing the disease (n=2234). All participants provided informed consent and the study protocol was approved by the regional research ethics committees for each clinical study center. Details of the study design and the core characteristics are explained elsewhere (13, 14).

### *Measures (IMI DIRECT)*

A T2\*-based multiecho technique was used to derive liver fat content from MRI (15, 16) and the percentage values were categorized into fatty ( $\geq 5\%$ ) or non-fatty concentrations ( $< 5\%$ ) to define the outcome variable. We elected not to attempt quantitative prediction of liver fat content, as this would require a much larger dataset to be adequately powered. A frequently-sampled 75g oral glucose tolerance test (OGTT) or a frequently sampled mixed-meal tolerance test (MMTT) was performed, from which measures of glucose and insulin dynamics were calculated, as previously described (13, 14, 17). Liver fat data were available for 1514 IMI DIRECT participants (503 diabetic and 1011 non-diabetic). The distribution of the liver fat data among different centers and cohorts is shown in S1 Fig and S2 Fig. The list of the clinical input (predictor) variables (n=58), including anthropometric, plasma biomarkers and lifestyle factors, are shown in S1 Table. These clinical variables were controlled for center effect by deriving residuals from a linear model including each clinical variable

per model; these residuals were then inverse normalized and used in subsequent analyses. A detailed overview of participant characteristics for the key variables is shown in Table 1 for all IMI DIRECT participants with MRI data. There were no substantial differences in characteristics between these participants and those from IMI DIRECT who did not have MRI data (see S2 Table).

Characteristics	Non-diabetic cohort		Diabetic cohort		Combined cohorts	
	Fatty	Non-fatty	Fatty	Non-fatty	Fatty	Non-fatty
N (%)	344 (34)	667 (66)	296 (59)	207 (41)	640 (42)	874 (58)
Age (yr)	61 (56, 66)	62 (56, 66)	62 (55, 67)	63 (58, 69)	61 (56, 66)	62 (56, 67)
Sex, n (% female)	62 (18)	134 (20)	130 (44)	86 (42)	192 (30)	220 (25)
Weight (kg)	90.75 (81.50, 100.25)	81.40 (75.67, 89.60)	92.85 (81.47, 103.75)	80.80 (73.00, 93.55)	91.20 (81.50, 102.00)	81.40 (74.03, 90.17)
Waist circ. (cm)	105 (98, 112)	97 (91, 103)	107 (97, 115)	97 (90, 107.25)	106 (98, 113)	97 (91, 103)
BMI (kg/m <sup>2</sup> )	29.23 (26.91, 32.05)	26.69 (24.75, 28.71)	31.47 (28.37, 35.35)	27.64 (25.53, 31.07)	30.05 (27.53, 33.52)	26.85 (24.91, 29.23)
SBP	134.70 (125.3, 143.0)	129.33 (120, 140)	131 (122, 139.33)	127.67 (117.67, 138.33)	132.67 (124.00, 142.00)	128.83 (119.33, 140.00)
DBP	83.50 (79.33, 89.83)	80.67 (75.67, 86.00)	76.67 (72, 84)	72.67 (67.17, 80.67)	81.33 (5.33, 87.33)	80.00 (73.33, 84.67)
HbA1c (mmol/mol)	38 (36, 40)	37 (35, 39)	47 (44, 51)	45 (42, 48)	41 (37, 46)	38 (36, 41)
Fasting glucose (mmol/L)	5.90 (5.60, 6.30)	5.70 (5.4, 6)	7.20 (6.3, 7.9)	6.70 (5.8, 7.6)	6.30 (5.8, 7.2)	5.80 (5.4, 6.3)
Fasting insulin (pmol/L)	75.60 (54.30, 104.40)	44.10 (27.75, 66.00)	115.8 (75.8, 167.8)	60.20 (40.85, 82.90)	90.90 (61.2, 133.9)	48.60 (30.00, 69.60)
2hr glucose (mmol/L)	6.55 (5.37, 8.20)	5.70 (4.70, 6.80)	9 (6.90, 10.65)	7.90 (6.20, 9.90)	7.40 (5.90, 9.60)	6 (4.90, 7.50)
2hr insulin (pmol/L)	345.60 (198.40, 566.20)	169.80 (100.2, 274.2)	489.30 (297.40, 700.50)	271 (166.40, 418.10)	403.20 (236.60, 643.50)	190.70 (110.80, 317.60)
Triglycerides (mmol/L)	1.49 (1.13, 2.09)	1.12 (0.86, 1.47)	1.49 (1.01, 1.99)	1.12 (0.86, 1.48)	1.49 (1.08, 2.02)	1.12 (0.86, 1.47)
ALT (U/L)	21 (14, 29)	15 (10, 20)	25 (19, 33.25)	20 (16, 24)	23 (16, 32)	16 (12, 22)
AST (U/L)	29 (24, 37)	25 (21, 29.75)	24 (20, 30)	22 (19, 27)	26 (22, 33)	24 (20, 29)
Alcohol intake, n ("never", "occasionally", "regularly")	21, 68, 255	91, 133, 443	52, 81, 163	38, 45, 124	73, 149, 418	129, 178, 567
Liver fat	8.80 (6.60, 13)	2.2 (1.50, 3.30)	11.10 (7.30, 15.82)	2.70 (1.95, 4)	9.5 (6.80, 14.30)	2.4 (1.60, 3.50)

**Table 1.** Characteristics of IMI DIRECT participants in the non-diabetes, diabetes and combined cohorts separated for fatty vs. non-fatty individuals. Values are median (interquartile range) unless otherwise specified.

Genetic, transcriptomic, proteomic, and metabolomic datasets were used as input omic variables in the analyses. Buffy coat was separated from whole blood, and DNA was



88 then extracted and genotyped using the Illumina HumanCore array (HCE24 v1.0);  
89 genotype imputation was performed using the Haplotype Reference Consortium (HRC)  
90 and 1000 Genome (1KG) reference panels. Details of the quality control (QC) steps for  
91 the genetic data are described elsewhere (14). Transcriptomic data were generated using  
92 RNA-sequencing from fasting whole blood. Only protein-coding genes were included  
93 in the analyses, as reads per kilobase of transcript per million mapped reads (RPKM).  
94 The targeted metabolomic data of fasting plasma samples were generated using the  
95 Biocrates Absolute*IDQ* p150 kit. Additionally, untargeted LC/MS-based metabolomics  
96 was used to cover a broader spectrum of metabolites. A combination of technologies  
97 and quantitative panels of protein assays were used to generate ‘targeted’ proteomic  
98 data. This included Olink’s proximity extension assays (18), sandwich immunoassay  
99 kits using Luminex technology (MerckMillipore and R&D Systems, Sweden),  
100 microfluidic ELISA assays (ProteinSimple, USA (19)), as well as protein analysis  
101 services from Myriad RBM (Myriad GmbH, Germany) and for hsCRP (MLM Medical  
102 Labs GmbH, Germany). In addition, protein data were generated by single-binder  
103 assays using highly multiplexed suspension bead arrays (20). This approach (denoted  
104 ‘exploratory’ proteomics) included a combination of antibodies targeting proteins  
105 selected by the consortium given published and unpublished evidence for association  
106 with glycemic-related traits. More information about data generation and QC of the  
107 transcriptomic, proteomic, and metabolomic data are described in the Supporting  
108 Information. Technical covariates for transcriptomics include *guanine-cytosine mean*  
109 *content, insert size, analysis lane* and *RNA integrity number, cell composition, date* and  
110 *center*. Technical covariates for proteomics were *center, assay, plate number* and *plate*  
111 *layout* (n=4), and for the targeted metabolites the technical covariates were *center* and

*plate*. These technical covariates were used to correct the omics data and the residuals were then extracted from these models and inverse normalized prior to further analyses.

# *Feature selection (IMI DIRECT)*

We developed a series of NAFLD prediction models, comprised of variables that are available within clinical settings, as well as those not currently available in most clinics (see S3 Table). We had two strategies for selecting the clinical variables: i) we selected variables based on the clinical-accessibility and their established association with fatty liver from existing literature without applying statistical procedures for data reduction (models 1-3); ii) a pairwise Pearson correlation matrix was used for feature selection of the clinical variables by placing a pairwise correlation threshold of  $r > 0.8$ . We then selected the variables we considered most accessible among those that were collinear (model 4). Feature selection was undertaken in the combined cohort (diabetic and non-diabetic) in order to maximize sample size and statistical power. Of 1514 participants with liver fat data, 1049 had all necessary clinical and multi-omics data for a complete case analysis. We used k-nearest neighbors (k-NN) (21) imputation method with k equal to 10 as a means to reduce the loss of sample size but found that this did not materially improve predictive power in subsequent analyses and determined not to include these imputed data. An overview of the pairwise correlations among the clinical variables available in 1049 IMI DIRECT Study participants is presented in Fig 1. The abbreviations used for the variables in the figure are defined in S1 Table.

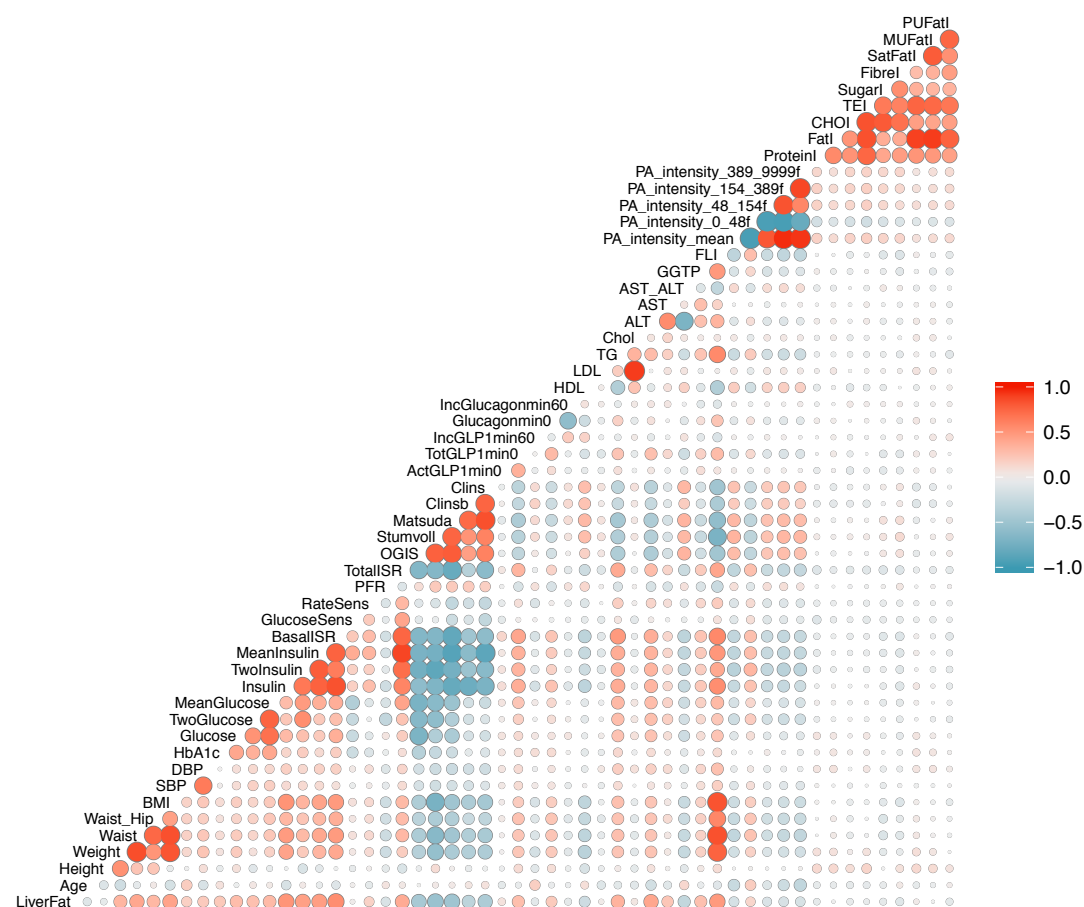


**Fig 1.** Pearson pairwise correlation matrix of clinical variables (data are inverse normal transformed) in the cohort combining participants with or without diabetes in IMI DIRECT (n=1049). The magnitude and direction of the correlation are reflected by the size (larger is stronger) and color (red is positive and blue is negative) of the circles respectively. The abbreviations used for the variables in the figure are defined in S1 Table.

The high-dimensionality nature of omics data also necessitated data reduction using the feature selection tool LASSO prior to building the model. LASSO is a regression analysis method that minimizes the sum of least squares in a linear regression model

and shrinks selected beta coefficients ( $\beta_j$ ) using penalties (formula (1)). Minimizing the following value, LASSO excludes the least informative variables and selects those features of most importance for the outcome of interest ( $y$ ) in a sample of  $n$  cases, each of which consists of  $m$  parameters. The penalty applied by  $\lambda$  can be any value from zero to positive infinity and is determined through a cross-validation step (22).

$$\sum_{i=1}^n (y_i - \hat{y}_i)^2 + \lambda \times \sum_{j=1}^m |\beta_j| \quad (1)$$

To minimize bias (for example by overfitting), we randomly divided the dataset and used 70% ( $n=735$ ) for feature selection and 30% ( $n=314$ ) for the model generation (see below). We selected these thresholds for partitioning the dataset in order to maximize the power to select the informative features. Stratified random sampling (23) based on the outcome variable was undertaken in order to preserve the distribution of the liver fat categories in the two feature selection and model generation sets. We selected LASSO, as a non-linear data reduction tool might lead to overfitting owing to the high dimensionality of omics data. LASSO was conducted with package glmnet in R (24) with a ten-fold cross-validation step for defining the  $\lambda$  parameter that results in the minimum value for the mean square error of the regression model.

Feature selection using LASSO was undertaken in each omics dataset (genetic, transcriptomic, proteomic and metabolomic) using 70% of the available data (models 5-18). For the genetic dataset, we first performed a genome-wide association study (GWAS) prior to LASSO in order to identify single-nucleotide polymorphisms (SNPs) tentatively associated with liver fat accumulation ( $P < 5 \times 10^{-6}$ ). LASSO was then applied to these index variants for feature selection in 70% of the study sample. The individual SNP association analysis was conducted with rvTests v2.0.2 (25), which

applies a linear mixed-model with an empirical kinship matrix to account for familial relatedness, cryptic relatedness, and population stratification. Only common variants with minor allele frequency (MAF) greater than 5% contributed to the kinship matrix. Liver fat data was log-transformed and then adjusted for age, age<sup>2</sup>, sex, center, body mass index (BMI) and alcohol consumption. These values were then inverse normal transformed and used in the GWAS analyses. S3 Fig and S4 Fig show the resulting Manhattan plot, depicting each SNP's association with liver fat percentage and the quantile-quantile (QQ) plot of the GWAS results for liver fat. For the genetic data, 46 SNPs were selected out of the 623 SNPs with p-values  $< 5 \times 10^{-6}$ . For the transcriptomics, 93 genes were selected out of 16,209 protein-coding genes. In the exploratory and targeted proteomics, 22 out of 377 and 48 out of 483 proteins were selected, respectively. In the targeted and untargeted metabolomic data, 39 out of 116 and 48 out of 172 were selected by LASSO, respectively.

### *Model training and evaluation*

The remaining 30% of the data was used to develop the binary prediction models for fatty liver (yes/no) with selected features used as input variables. We utilized the Random Forest supervised machine learning method, which is an aggregation of decision trees built from bootstrapped datasets (a process called 'bagging'). Typically, two-thirds of the data are retained in these bootstrapped datasets and the remaining third is termed the 'out of bag' dataset (*OOB*), the latter of which is used to validate the performance of the model. To avoid over-fitting and improve generalizability, five-fold cross-validation was done for resampling the training samples and was repeated 5 times to create multiple versions of the folds. The number of trees was set to 1000 to provide an accurate and stable prediction. Receiver Operator Characteristic (ROC) curves were

used to evaluate model performance by measuring the area under the curve (AUC). A ROC curve uses a combination of *sensitivity* (true positive rate) and *specificity* (true negative rate) to assess prediction performance. In our analysis, the Random Forest model is used to derive probability estimates for the presence of fatty liver. In order to make a class prediction, it is necessary to impose a cut-off above which fatty liver is deemed probable and below which it is considered improbable. The choice of cut-off influences both sensitivity and specificity for a given prediction model. We considered the effect of different cut-offs on these performance measurements. Additionally, we calculated the *F1 score* (26), which is the harmonic mean of precision (positive predictive value) and sensitivity, derived as follows:

$$F1 \text{ score} = \frac{2 \times \text{sensitivity} \times \text{precision}}{(\text{sensitivity} + \text{precision})} \quad (2)$$

*Balanced Accuracy* was also evaluated, which is the proportion of individuals correctly classified (true positives and true negatives) within each class individually. Measurements of sensitivity, specificity, F1 score and balanced accuracy were computed and compared at different cut-offs for diabetic, non-diabetic and the combined cohorts. The variable importance was also determined via a “permutation accuracy importance” measure using Random Forest. In brief, for each tree, the prediction accuracy was calculated in the OOB test data. Each predictor variable was then permuted and the accuracy was recalculated. The difference in the accuracies was averaged over all the trees and then normalized by the standard error. Accordingly, a measure for variable importance is the difference in prediction accuracy before and after the permutation for each variable (27). Statistical analyses were undertaken using R software version 3.2.5 (28) and the Random Forest models were built using the Caret package (29). Fig 2 shows an overview of the different stages involved in the data processing and model training.

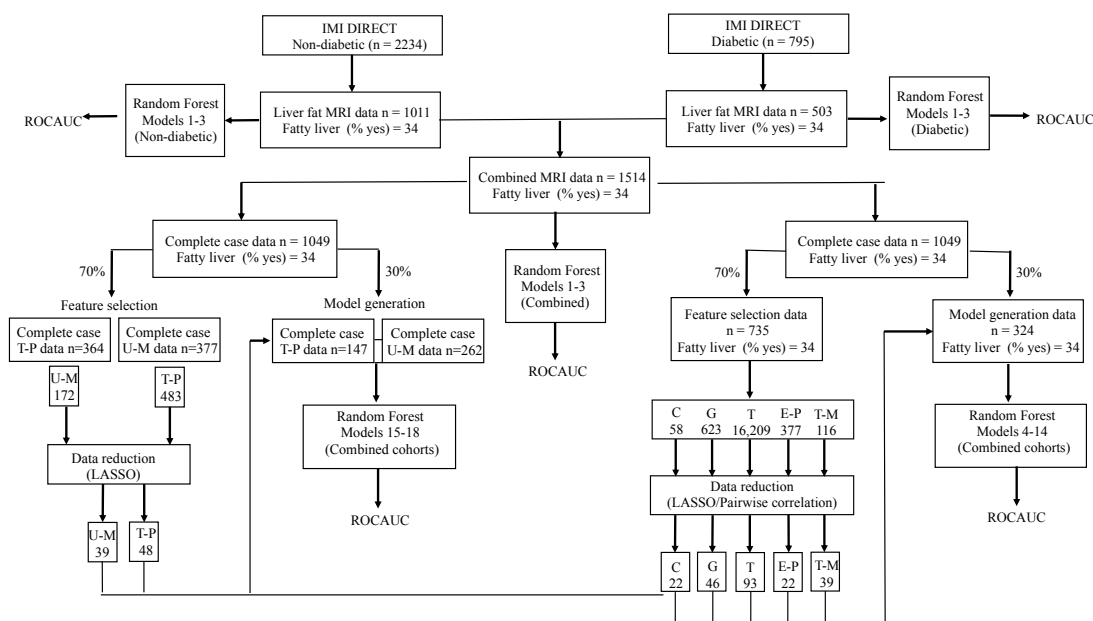


**Fig 2.** Overview of the different stages involved in data processing and model training: Clinical (C), Genetic (G), Transcriptomic (T), Exploratory Proteomic (E-P), Targeted Proteomic (T-P), Targeted Metabolomic (T-M) and Untargeted Metabolomic (U-M).

### Comparison with other fatty liver indices

Given the accessible data within the IMI DIRECT cohorts, several existing fatty liver indices could be calculated and compared with the IMI DIRECT prediction models. These included the *fatty liver index (FLI)* (30), *hepatic steatosis index (HSI)* (31) and *NAFLD liver fat score (NAFLD-LFS)* (32).

### FLI

The FLI is commonly used to estimate the presence or absence of fatty liver (categorized into fatty ( $\geq 60$ ) or non-fatty liver ( $< 60$ ) FLI units) (30). FLI uses data on plasma triglycerides (TG), waist circumference, BMI and serum gamma-glutamyl transpeptidase (GGTP) and is calculated as follows:

$$FLI = \frac{e^{((0.953 \times \ln(TG)) + (0.139 \times BMI) + (0.718 \times \ln(GGTP)) + (0.053 \times Waist) - 15.745)} \times 100}{(1 + e^{((0.953 \times \ln(TG)) + (0.139 \times BMI) + (0.718 \times \ln(GGTP)) + (0.053 \times Waist) - 15.745)})} \quad (3)$$

236

237 NAFLD-FLS

238 NAFLD-FLS was calculated using fasting serum (fs) insulin, aspartate transaminase  
239 (AST), alanine transaminase (ALT), T2D and metabolic syndrome (MS) (defined  
240 according to the International Diabetes Federation (33)) to provide an estimate of liver  
241 fat content. A NAFLD-FLS value above -0.64 is considered to indicate the presence of  
242 NAFLD:

$$243 \quad \text{NAFLD-FLS} = -2.89 + 1.18 \times \text{MS (yes 1, no 0)} + 0.45 \times \text{T2D (yes 2, no 0)} + 0.15 \times \text{fs Insulin} \quad (4)$$

244

245 HSI

246 The HSI uses BMI, sex, T2D diagnosis (yes/no) and the ratio of ALT to AST and  
247 calculated as follows:

$$248 \quad \text{HSI} = 8 \times \frac{\text{ALT}}{\text{AST}} + \text{BMI} (+2 \text{ if T2D yes, } +2 \text{ if female}) \quad (5)$$

249 HSI values above 36 are deemed to indicate the presence of NAFLD.

250

251 *External validation (UK Biobank cohort)*

252 The UK Biobank cohort (34) was used to validate the clinical prediction models  
253 (models 1 and 2) derived using IMI DIRECT data (UK Biobank application ID: 18274).

254 The same protocol and procedure have been used to quantify MRI-derived liver fat in  
255 IMI DIRECT and UK Biobank (16). In addition, we validated the FLI and HSI using  
256 UK Biobank data. Field numbers for the UK Biobank variables used in the validation  
257 step can be found in the S4 Table. The data analysis procedures used for the UK  
258 Biobank validation analyses mirror those used in IMI DIRECT (as described above).

259



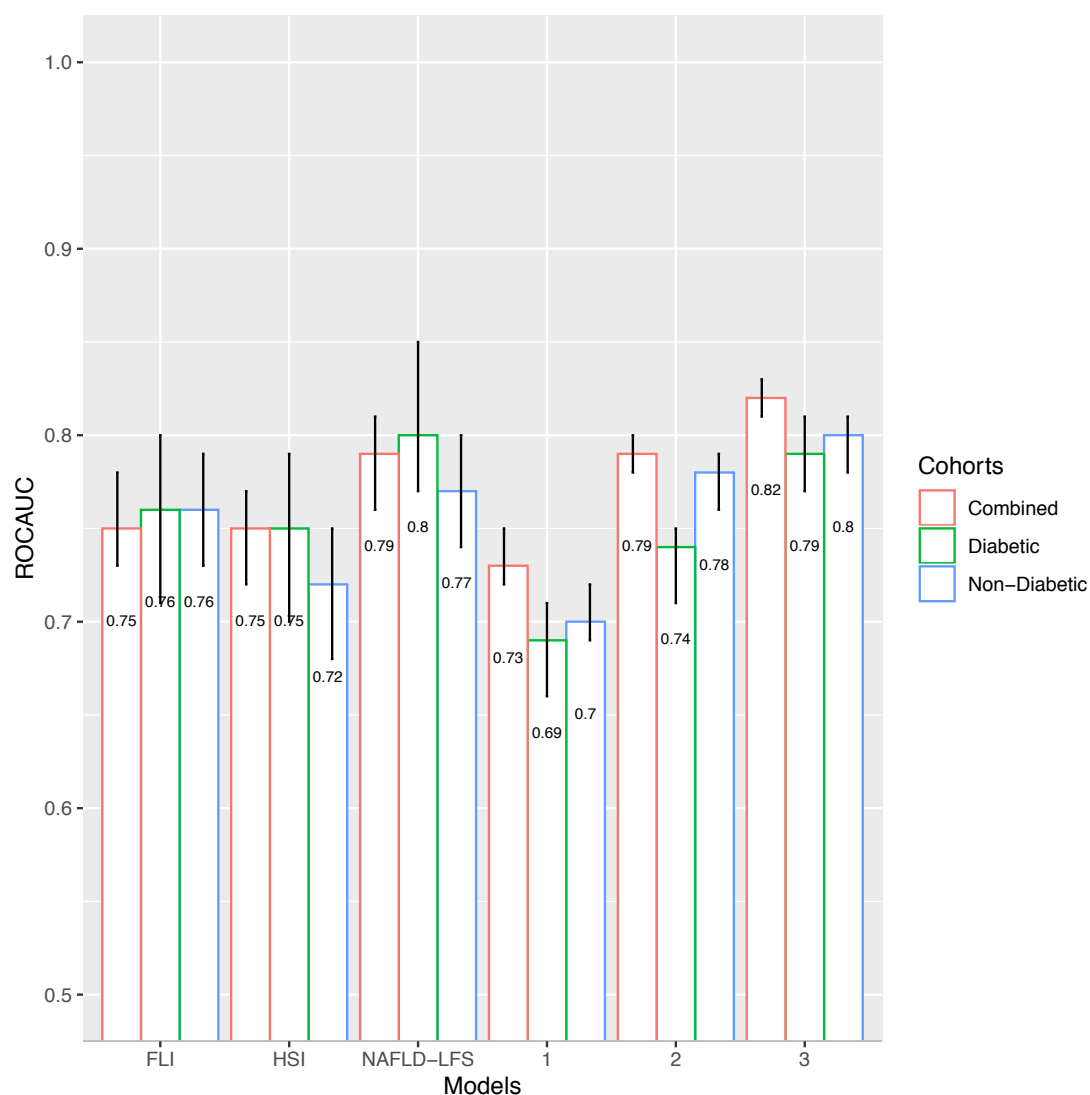
## RESULTS

The following section describes fatty liver prediction models that are likely to suit different scenarios. We focus on a basic model (model 1), which includes variables that are widely available in both clinical and research settings. Models 2 and 3 focus on variables that could in principle be accessed within the clinical context, but which are not routinely available in the clinical setting at this time. Model 4 includes clinical variables, more detailed measures of glucose and insulin dynamics, and physical activity. Models 5 to 18 are more advanced models that include omic predictor variables alone or in combination with clinical predictor variables. See S3 Table for a full description of models.

### *Clinical models (Models 1-3)*

We developed models 1-3 for NAFLD prediction, graded by perceived data accessibility for clinicians. These models were developed on the full dataset without applying any statistical procedures for feature selection. Model 1 includes six non-serological input variables: waist circumference, BMI, systolic blood pressure (SBP), diastolic blood pressure (DBP), alcohol consumption and diabetes status. Model 2 includes eight input variables: waist circumference, BMI, TG, ALT, AST, fasting glucose (or hemoglobin A1C (HbA1c) if fasting glucose is not available), alcohol consumption and diabetes status. Model 3 includes nine variables: waist circumference, BMI, TG, ALT, AST, fasting glucose, fasting insulin, alcohol consumption and diabetes status. The three clinical models along with FLI, HSI and NAFLD-LFS indices were applied to the non-diabetic and diabetic cohort datasets separately, as well as in the combined dataset; the ROCAUC results are presented in Fig 3. Model 1 yielded a ROCAUC of 0.73 (95% confidence interval (CI)=0.72, 0.75) in both cohorts combined.

285 Adding serological variables to model 2 (with either fasting glucose or HbA1c) for the  
 286 combined cohorts yielded the ROCAUC of 0.79 (95% CI=0.78, 0.80). Model 3 (fasting  
 287 insulin added) yielded a ROCAUC of 0.82 (95% CI=0.81, 0.83) in the combined  
 288 cohorts. The FLI, HSI and NAFLD-LFS had the ROCAUCs of 0.75 (95% CI=0.73,  
 289 0.78), 0.75 (95% CI=0.72, 0.77) and 0.79 (95% CI=0.76, 0.81) in the combined cohorts,  
 290 respectively. The predictive performance of the clinical models 1-3, FLI, HSI and  
 291 NAFLD-LFS in the non-diabetes and diabetes cohorts are presented in S5 Table.



292  
 293 **Fig 3.** Receiver operator characteristic area under the curve (ROCAUC) with 95%  
 294 confidence intervals (error bars) for the clinical models 1-3, FLI, HSI and NAFLD-LFS  
 295 (x-axis) in the IMI DIRECT cohorts. Model 1 includes six non-serological input

variables: waist circumference, BMI, SBP, DBP, alcohol consumption and diabetes status. Model 2 includes eight input variables: waist circumference, BMI, TG, ALT, AST, fasting glucose (or hemoglobin A1C (HbA1c) if fasting glucose is not available), alcohol consumption and diabetes status. Model 3 includes nine variables: waist circumference, BMI, TG, ALT, AST, fasting glucose, fasting insulin, alcohol consumption and diabetes status.

### *Performance metrics*

We further investigated sensitivity, specificity, balanced accuracy and F1 score (a score considering sensitivity and precision combined) metrics. These measurements were calculated for different cut-offs applied to the output of the Random Forest model (0.1, 0.2, 0.3, 0.4, 0.5, 0.6, 0.7, 0.8 and 0.9) using the clinical models (models 1-3) in the diabetic, non-diabetic and the combined cohorts. The performance metrics for models 1 and 2 are presented in S5 Fig and S6 Fig and for model 3 the metrics are presented in Fig 4. We aimed to find the optimal cut-off for these models based on the cross-validated balanced accuracy. The highest balanced accuracy for models 1-3 in the non-diabetic, diabetic and combined cohorts were observed at cut-offs of 0.4, 0.6 and 0.4, respectively (see Table 2).

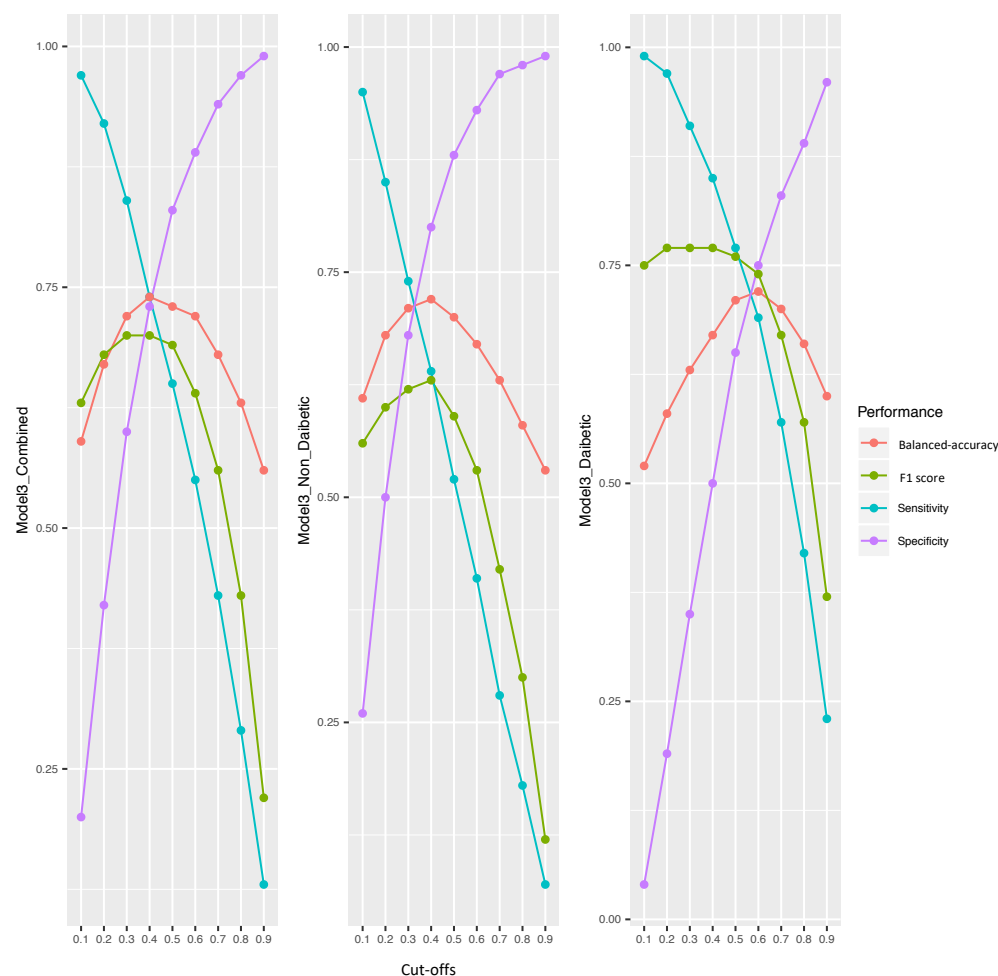


**Fig 4.** Measurements of F1, sensitivity, specificity and balanced accuracy (y-axis) at different cut-offs (x-axis) for model 3 in the diabetic, non-diabetic and the combined cohorts of the IMI-DIRECT. The measurements are calculated by defining the predicted probabilities of fatty liver equal or above these cut-offs as fatty and below as non-fatty.

Measurements of sensitivity, specificity, F1 score and balanced accuracy were computed for FLI, HSI and NAFLD-LFS indices and compared with those of the clinical models (1-3). These measurements were computed at the optimal cut-off values for these indices: -0.640 for NAFLD-LFS; 60 for FLI and 36 for HSI, respectively. A comprehensive overview of the prediction models' performance metrics for all of the fatty liver indices listed above is shown in Table 2.

Model	Cut-off	Sensitivity	Specificity	F1 score	Balanced-accuracy
<b>Non-diabetic (IMI DIRECT)</b>					
1	0.4	0.51	0.75	0.51	0.63
2	0.4	0.60	0.79	0.59	0.69
3	0.4	0.64	0.80	0.63	0.72
FLI	60	0.89	0.41	0.58	0.65
HSI	36	0.62	0.68	0.55	0.65
NAFLD-LFS	-0.64	1	0.04	0.51	0.52
<b>Diabetic (IMI DIRECT)</b>					
1	0.6	0.63	0.64	0.67	0.64
2	0.6	0.65	0.68	0.69	0.67
3	0.6	0.69	0.75	0.74	0.72
FLI	60	0.77	0.54	0.73	0.66
HSI	36	0.83	0.48	0.75	0.65
NAFLD-LFS	-0.64	1	0.01	0.73	0.50
<b>Combined (IMI DIRECT)</b>					
1	0.4	0.67	0.65	0.62	0.66
2	0.4	0.72	0.69	0.67	0.71
3	0.4	0.74	0.73	0.70	0.74
FLI	60	0.84	0.44	0.64	0.64
HSI	36	0.71	0.63	0.64	0.67
NAFLD-LFS	-0.64	1	0	0.58	0.50
<b>UK Biobank</b>					
1	0.4	0.49	0.78	0.43	0.63
2	0.4	0.67	0.74	0.52	0.71
FLI	60	0.62	0.76	0.50	0.69
HSI	36	0.66	0.72	0.50	0.69

326

327 **Table 2:** An overview of the prediction models' performance metrics for all of the fatty  
328 liver indices in the IMI DIRECT and UK Biobank datasets

329

330 *Validation in UK Biobank and IMI DIRECT*

331 Liver fat data were available in 4617 UK Biobank participants (1011 with  $\geq 5\%$  and  
332 3606 with  $< 5\%$  liver fat). Of these individuals, 4609 had all the required variables to  
333 replicate the clinical model 1. To perform model 2 either with fasting glucose or  
334 HbA1c, 3807 participants had data available for a complete case analysis. Given the  
335 limited availability of variables in the UK Biobank dataset, only models 1 and 2 of the  
336 NAFLD prediction models we developed could be externally validated. To facilitate  
337 this validation analysis, the Random Forest models developed in the IMI DIRECT  
338 cohorts were used to predict the liver fat category (fatty vs. non-fatty) for the UK  
339 Biobank participants. The performance of FLI and HSI was also tested in the UK  
340 Biobank cohort. We validated both models 1 and 2 in the UK Biobank cohort with a  
341 similar ROCAUC as seen in the IMI DIRECT dataset. The ROCAUCs were 0.71 (95%  
342 CI= 0.69, 0.73), 0.79 (95% CI= 0.77, 0.80), and 0.78 (95% CI= 0.76, 0.79), for model  
343 1 and model 2 (with fasting glucose or with HbA1c), respectively. The FLI had a  
344 ROCAUC of 0.78 (95% CI= 0.76, 0.80), which is similar to model 2. The HSI yielded  
345 a ROCAUC of 0.76 (95% CI= 0.75, 0.78).

346 Measurements of sensitivity, specificity, F1 score and balanced accuracy were also  
347 computed at the optimal cut-off values for these models: 0.4 for clinical models 1 and  
348 2; 60 for FLI; 36 for HSI, respectively (see Table 2).

349

350

351 *Omics models separately or in combination with clinical variables (models 5-14)*

352 More advanced models using omics data were also developed. These models were

353 generated using the omics features selected by LASSO in the combined cohorts. The

354 models include only omics or include omics plus 22 clinical variables as the input

355 variables. These clinical variables, selected based on the pairwise Pearson correlation

356 matrix, are: BMI, waist circumference, SBP, DBP, alcohol consumption, ALT, AST,

357 GGTP, HDL, TG, fasting glucose, 2-hour glucose, HbA1c, fasting insulin, 2-hour

358 insulin, insulin secretion at the beginning of the carbohydrate challenge tests (OGTT or

359 MMTT), insulin sensitivity 2-hour OGIS, mean insulin clearance during the

360 OGTT/MTT, fasting glucagon concentration, fasting plasma total GLP-1

361 concentration, and mean physical activity intensity. Diabetes status (non-

362 diabetic/diabetic) was also included as a clinical predictor in the models, given that

363 analyses were undertaken in the combined diabetic and non-diabetic cohorts. The

364 ROCAUCs for these models (models 4-14) are shown in Fig 5. The clinical model with

365 the 22 selected clinical variables (model 4) yielded in ROCAUC of 0.79 (95% CI= 0.76,

366 0.81). Omics models with only the genetic (model 5), transcriptomic (model 7),

367 proteomic (model 9) and targeted metabolomic (model 11) data as input variables

368 resulted in ROCAUCs of 0.69 (95% CI= 0.66, 0.71), 0.72 (95% CI= 0.69, 0.74), 0.74

369 (95% CI= 0.71, 0.76) and 0.70 (95% CI= 0.67, 0.72), and respectively. Including all

370 the omics variables in one model (model 13) resulted in a ROCAUC of 0.81 (95% CI=

371 0.76, 0.84). Adding the clinical variables to each omics model improved the prediction

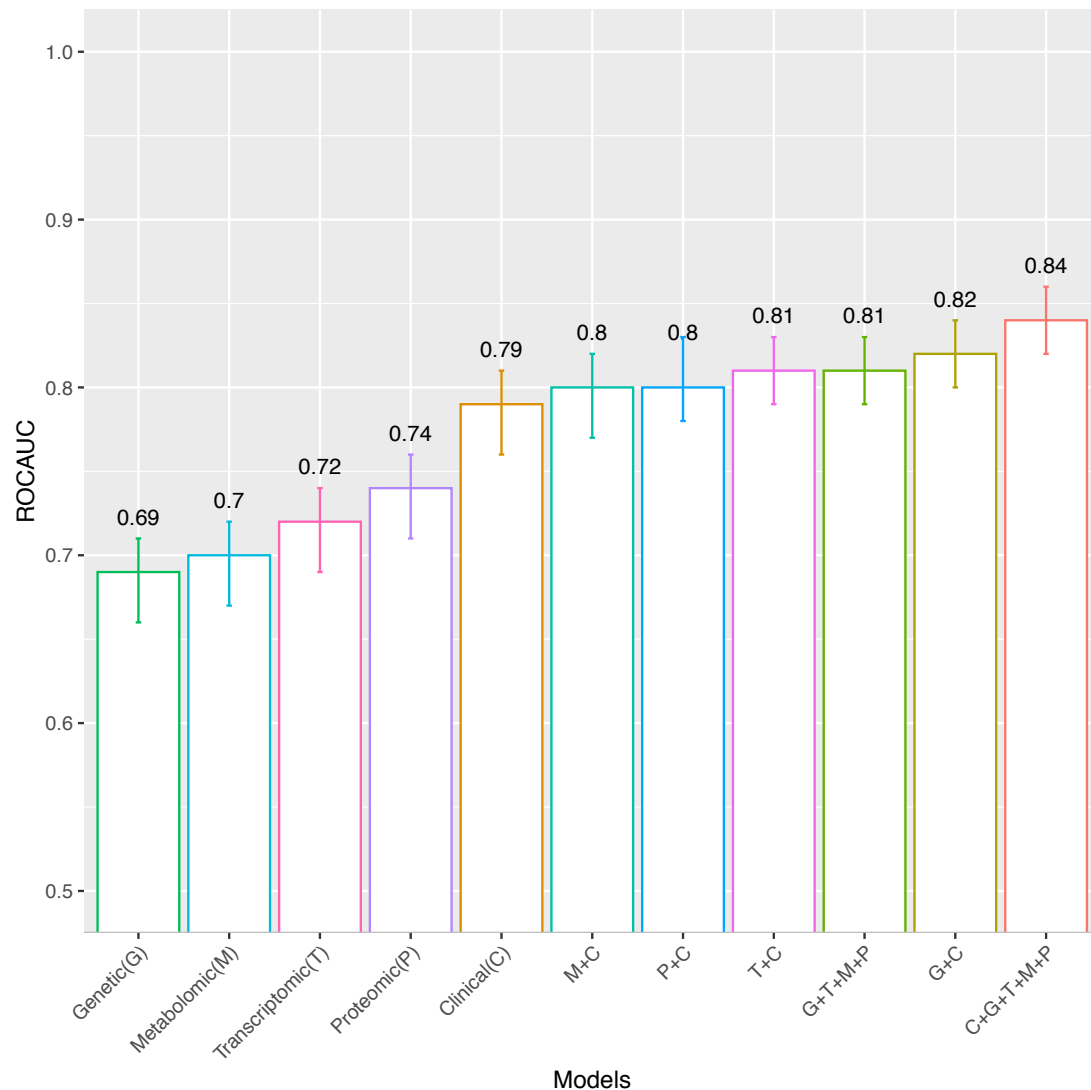
372 ability; models with the clinical variables plus genetic (model 6), transcriptomic (model

373 8), exploratory proteomic (model 10) and targeted metabolomic (model 12) resulted in

374 ROCAUCs of 0.82 (95% CI= 0.80, 0.84), 0.81 (95% CI= 0.79, 0.83), 0.80 (95% CI=

375 0.78, 0.83) and 0.80 (95% CI= 0.77, 0.82), respectively. The highest performance was

376 observed for model 14 (ROCAUC of 0.84, 95% CI= 0.82, 0.86). The variable  
377 importance for model 14 is presented in Fig 6, which shows that measures of insulin  
378 secretion rank amongst the highest of all input variables. Rankings for the individual  
379 clinical and omics variables are presented in S7-13 Figs.



380  
381 **Fig 5.** Receiver operator characteristic area under the curve (ROCAUC, y-axis) with  
382 95% confidence intervals (error bars) for the Clinical model (C) with the 22 selected  
383 clinical variables (model 4), for the omics models separately (Genetic (G) (model 5),  
384 Transcriptomic (T) (model 7), Exploratory Proteomic (P) (model 9) and Targeted  
385 Metabolomic (M) (model 11)), for all omics together (G+T+M+P)(model 13) and for  
386 omics combined with the clinical model (C+G (model 6), C+T (model 8), C+P (model



10), C+M (model 12) and C+G+T+M+P (model 14)) in the cross-validated test data of IMI DIRECT combined cohorts.

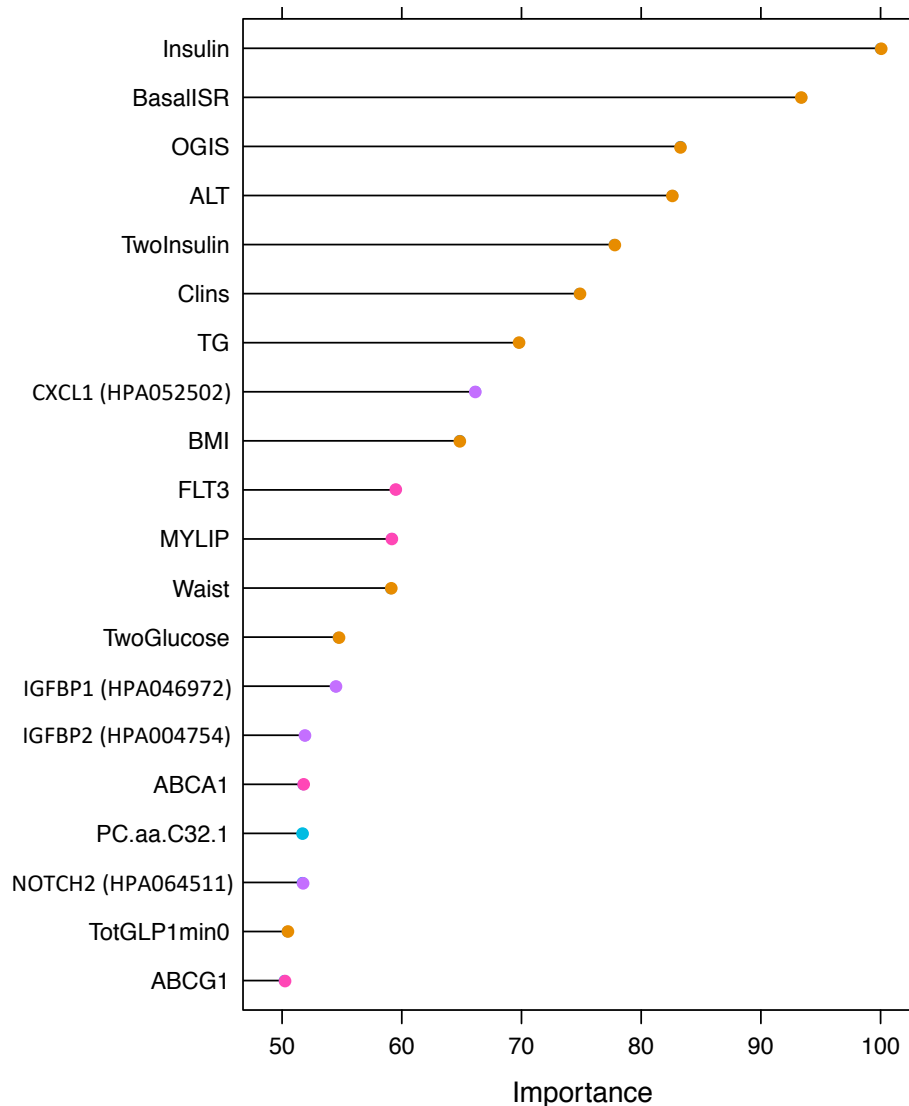


**Fig 6.** Variable importance for the Advanced model 14 with 222 omics and clinical input variables (clinical=22, genetic=46, transcriptomic=93, exploratory proteomic=22 and targeted metabolomic=39). The y-axis shows the top 20 predictors in the model. The x-axis shows the variable importance, calculated via a “permutation accuracy importance” measure using Random Forest as the difference in prediction accuracy before and after the permutation for each variable scaled by the standard error.

398

### 399 *Additional proteomic and metabolomic analyses (models 15-18)*

400 Data from targeted proteomics and untargeted metabolomic data were further utilized  
 401 to develop the omics models separately or in combination with the clinical data.  
 402 However, as some participants lacked these omics data, their models were developed  
 403 using a smaller data subset and were, hence, not included in the advanced (model 14)  
 404 analyses. The complete case analysis was primarily defined on the availability of the  
 405 22 clinical variables (n=1049). Within this complete case set, 511 had a complete set  
 406 of untargeted metabolomics data and 686 had a complete set of targeted proteomics  
 407 data. Models with either targeted proteomic data only, or proteomic and clinical  
 408 variables combined resulted in ROCAUCs of 0.81 (95% CI=0.78, 0.84) and 0.84 (95%  
 409 CI=0.81, 0.87), respectively. The untargeted metabolomic model alone had a ROCAUC  
 410 of 0.66 (95% CI=0.63, 0.69), which increased to 0.78 (95% CI= 0.75, 0.80) when the  
 411 22 clinical variables were added.

412 A web interface for the diagnosis of NAFLD was developed using the findings  
 413 described above ([www.predictliverfat.org](http://www.predictliverfat.org)), which we anticipate will render the models  
 414 (1-3) developed here accessible for the wider community of clinicians and researchers.

## 415 **DISCUSSION**

416 Using data from the IMI DIRECT consortium, we developed 18 diagnostic models for  
 417 early-stage NAFLD. These models were developed to reflect different scenarios within  
 418 which they might be used: these included both clinical and research settings, with the  
 419 more complex (and less accessible) models having the greatest predictive ability. The  
 420 models were successfully validated in the UK Biobank, where data permitted. Overall,  
 421 the basic clinical variables proved to be stronger predictors of the fatty liver than more

complex omics data, although adding omics data yielded the most powerful model, with very good cross-validated predictive ability (ROCAUC=0.84).

NAFLD is etiologically complex, rendering its prevention and treatment difficult, and diagnosis can require invasive and/or relatively expensive procedures. Thus, non-invasive and cost-effective prediction models with good sensitivity and specificity are much needed. This is especially important because if NAFLD is detected early, treatment through lifestyle interventions can be highly effective (35). However, simple NAFLD is usually asymptomatic and many patients only come to the attention of hepatologists when serious complications arise (36).

To date, several prediction models have been developed to facilitate the diagnosis of steatosis (thoroughly reviewed elsewhere (11)). FLI is the most well-established and commonly used index, initially developed using ultrasound-derived hepatic steatosis data (30). The FLI yielded similar predictive performance in the diabetic and non-diabetic cohorts of IMI DIRECT (ROCAUC ~ 0.75).

Though commonly used for liver fat prediction, the FLI has a similar discriminative ability as waist circumference alone (37). Better discrimination can be obtained by incorporating additional serological and hemostatic measures, which is the case with the NAFLD-LFS (12), the SteatoTest (38) and the HSI (31), for example. Notwithstanding the added complexity and cost of these scores, the FLI, HSI and the NAFLD-LFS yielded similar predictive ability in a series of liver biopsy-diagnosed NAFLD cases (n=324) (32).

Omics technologies have been used in a small number of studies to identify molecular biomarkers of NAFLD (39-41). This includes tests utilizing genetic data such as FibroGENE for staging liver fibrosis (42), and tests using metabolomic data derived from liver tissue to differentiate simple hepatitis from NASH (43), as well as a multi-

447 component NAFLD classifier using genomic, proteomic and phenomic data (41). Using  
 448 data from IMI DIRECT, we explored the predictive ability of genetic, transcriptomic,  
 449 proteomic and metabolomic data from the blood for the diagnosis of NAFLD. The top  
 450 twenty features of each omic model are presented in the S7-13 Figs. The details of the  
 451 LASSO selected features are summarized in the Supporting Information (Excel file).  
 452 Reassuringly, several of the features that ranked highest have been previously described  
 453 for their association with liver fat content or closely related traits; this includes *PNPLA3*  
 454 gene variants (40, 44), fetal liver tyrosine kinase-3 (FLT3) transcripts (45), IGFBP1(46-  
 455 48) and Lipoprotein lipase (Lpl) (49) proteins, and the metabolite glutamate (50). In the  
 456 analysis of the targeted metabolites, phosphatidylcholines, including PC.aa.C32,  
 457 PC.aa.C38, PC.aa.C40 and PC.aa.C42, glycerophospholipids and valine were amongst  
 458 the highest-ranked metabolites that are known for their correlation with NAFLD and  
 459 metabolic disorders (51, 52). For exploratory proteomics, the most important variables  
 460 were proteins secreted into the blood, expressed by the liver as well as those leaking  
 461 from the blood cells (53). The prediction model that only included targeted proteomic  
 462 data (model 15) performed well (ROCAUC=0.81), rendering it an interesting candidate  
 463 biomarker for future clinical tests. Among the top 20 most important proteins were  
 464 many secreted into blood or leaked by the liver, as well as the pancreas, fat or muscle  
 465 tissue (54).

466 The models developed here may be used for screening. In order to stratify people likely  
 467 to have NAFLD who might then undergo more invasive and/or costly assessments, it  
 468 would be necessary for the prediction model to have high sensitivity. However, the  
 469 predictive utility of a given model can be further improved, by selecting model cut-offs  
 470 that optimize sensitivity or specificity, as the two metrics rarely perform optimally at  
 471 the same cut-off. This issue was apparent for models 1-3 in the current analyses, where

we selected cut-offs that maximize balanced accuracy (considering both sensitivity and specificity); these features are especially important in screening algorithms, where the cost of false negatives can be high. Models 1-3 resulted in higher sensitivity in the diabetic cohort than the non-diabetic cohort, whereas the specificity was higher in the non-diabetic and in both cohorts combined than in the diabetic cohort.

It is noteworthy that the analytical methods deployed here required a complete case analysis, which diminishes sample size considerably and is, thus, a limitation of this approach; although imputing missing data here helped preserve sample size, it did not improve the prediction ability of the models, and we hence elected to use the complete case analysis. The linear Lasso method was used to minimize overfitting that can occur with high-dimensionality data, while Random Forests was used to identify non-linear associations where data structure allowed.

Heavy alcohol consumption is a key determinant of fatty liver but is unlikely to be a major etiological factor in IMI DIRECT owing to the demographics of this cohort. Nevertheless, a further limitation of this analysis is that alcohol intake was self-reported and may lack validity. To address this limitation, we removed all self-reported heavy alcohol consumers from the UK Biobank cohort and undertook sensitivity analyses, but this did not materially affect the results. A further consideration for future work is the impact lifestyle and medications are likely to have on the prediction of NAFLD. Here we considered lifestyle variables, but not medications. However, the use of medicines affecting liver fat is likely to be less in the non-diabetic than in the diabetic cohorts, yet the models fit better in the latter, suggesting that glucose-lowering medication use in the DIRECT cohorts does not have a major detrimental impact on prediction model performance.

In summary, we have developed prediction models for NAFLD that may have utility for clinical diagnoses and research investigations alike. Our finding that a model focused on proteomic data yielded high predictive utility may warrant further investigation. Our analysis also suggests that insulin sensitivity and beta-cell dysfunction may be involved in liver fat accumulation, which are at present not considered as features of conventional NAFLD risk models.

## **ACKNOWLEDGMENTS**

We thank Mattias Borell for developing, logistical support and advice related with the web interface. We thank all the participants and study center staff in IMI DIRECT for their contribution to the study. We thank all the participants in the UK Biobank. This research was conducted using the UKBB Resource (application ID: 18274). For the proteomics analyses, we thank the entire staff of the Human Protein Atlas, the Plasma Profiling facility at Science for Life Laboratory and in particular Elin Birgersson, Annika Bendes, and Eni Andersson for technical assistance

## REFERENCES

1. Tilg H, Moschen AR. Insulin resistance, inflammation, and non-alcoholic fatty liver disease. *Trends Endocrinol Metab.* 2008;19(10):371-9.
2. Sattar N, Gill JM. Type 2 diabetes as a disease of ectopic fat? *BMC Med.* 2014;12:123.
3. Sattar N, Forrest E, Preiss D. Non-alcoholic fatty liver disease. *BMJ.* 2014;349:g4596.
4. Lucas C, Lucas G, Lucas N, Krzowska-Firych J, Tomasiewicz K. A systematic review of the present and future of non-alcoholic fatty liver disease. *Clin Exp Hepatol.* 2018;4(3):165-74.
5. Fazel Y, Koenig AB, Sayiner M, Goodman ZD, Younossi ZM. Epidemiology and natural history of non-alcoholic fatty liver disease. *Metabolism.* 2016;65(8):1017-25.
6. Bellentani S. The epidemiology of non-alcoholic fatty liver disease. *Liver Int.* 2017;37 Suppl 1:81-4.
7. Younossi ZM, Koenig AB, Abdelatif D, Fazel Y, Henry L, Wymer M. Global epidemiology of nonalcoholic fatty liver disease-Meta-analytic assessment of prevalence, incidence, and outcomes. *Hepatology.* 2016;64(1):73-84.
8. Younossi ZM. Non-alcoholic fatty liver disease - A global public health perspective. *J Hepatol.* 2019;70(3):531-44.
9. Younossi ZM, Tampi R, Priyadarshini M, Nader F, Younossi IM, Racila A. Burden of Illness and Economic Model for Patients With Nonalcoholic Steatohepatitis in the United States. *Hepatology.* 2019;69(2):564-72.
10. Castera L, Friedrich-Rust M, Loomba R. Noninvasive Assessment of Liver Disease in Patients With Nonalcoholic Fatty Liver Disease. *Gastroenterology.* 2019;156(5):1264-81 e4.
11. Castera L. Diagnosis of non-alcoholic fatty liver disease/non-alcoholic steatohepatitis: Non-invasive tests are enough. *Liver Int.* 2018;38 Suppl 1:67-70.
12. Kotronen A, Peltonen M, Hakkarainen A, Sevastianova K, Bergholm R, Johansson LM, et al. Prediction of non-alcoholic fatty liver disease and liver fat using metabolic and genetic factors. *Gastroenterology.* 2009;137(3):865-72.
13. Koivula RW, Heggie A, Barnett A, Cederberg H, Hansen TH, Koopman AD, et al. Discovery of biomarkers for glycaemic deterioration before and after the onset of type 2 diabetes: rationale and design of the epidemiological studies within the IMI DIRECT Consortium. *Diabetologia.* 2014;57(6):1132-42.
14. Koivula RW, Forgie IM, Kurbasic A, Vinuela A, Heggie A, Giordano GN, et al. Discovery of biomarkers for glycaemic deterioration before and after the onset of type 2 diabetes: descriptive characteristics of the epidemiological studies within the IMI DIRECT Consortium. *Diabetologia.* 2019;62(9):1601-15.
15. Thomas EL, Fitzpatrick JA, Malik SJ, Taylor-Robinson SD, Bell JD. Whole body fat: content and distribution. *Prog Nucl Magn Reson Spectrosc.* 2013;73:56-80.
16. Wilman HR, Kelly M, Garratt S, Matthews PM, Milanese M, Herlihy A, et al. Characterisation of liver fat in the UK Biobank cohort. *PLoS One.* 2017;12(2):e0172921.
17. Robert W. Koivula IF, Azra Kurbasic, Ana Vinuela, Alison Heggie, Tue Hansen, Michelle Hudson, Anitra Koopman, Femke Rutters, Maritta Siloaho,



Søren Brage, Adem Y. Dawed, Heather Ford, Giuseppe N. Giordano, Christopher J. Groves, Tarja Kokkola, Anubha Mahajan, Mandy H. Perry, Simone P. Rauh, Martin Ridderstråle, Harriet J. A. Teare, Louise Thomas, Andrea Tura, Henrik Vestergaard, Tom White, Jerzy Adamski, Jimmy Bell, Søren Brunak, Jacqueline Dekker, Emanouille Dermitzakis, Philippe Froguel, Gary Frost, Ramneek Gupta, Torben Hansen, Andrew Hattersley, Bernd Jablonka, Markku Laakso, Timothy J. McDonald, Oluf Pedersen, Andrea Mari, Mark I. McCarthy, Hartmut Ruetten, Imre Pavo, Mark Walker, Ewan Pearson, Paul W. Franks, for the IMI DIRECT consortium. Discovery of biomarkers for glycaemic deterioration before and after the onset of type 2 diabetes: an overview of the baseline data from the epidemiological studies within the IMI DIRECT Consortium. *Diabetologia*. 2018.

18. Assarsson E, Lundberg M, Holmquist G, Björkstén J, Thorsen SB, Ekman D, et al. Homogenous 96-plex PEA immunoassay exhibiting high sensitivity, specificity, and excellent scalability. *PLoS One*. 2014;9(4):e95192.
19. Aldo P, Marusov G, Svancara D, David J, Mor G. Simple Plex() : A Novel Multi-Analyte, Automated Microfluidic Immunoassay Platform for the Detection of Human and Mouse Cytokines and Chemokines. *Am J Reprod Immunol*. 2016;75(6):678-93.
20. Drobin K, Nilsson P, Schwenk JM. Highly multiplexed antibody suspension bead arrays for plasma protein profiling. *Methods Mol Biol*. 2013;1023:137-45.
21. Altman NS. An Introduction to Kernel and Nearest-Neighbor Nonparametric Regression. *Am Stat*. 1992;46(3):175-85.
22. Tibshirani R. Regression Shrinkage and Selection via the Lasso. *Journal of the Royal Statistical Society*. 1996;Vol. 58.
23. Setia MS. Methodology Series Module 5: Sampling Strategies. *Indian J Dermatol*. 2016;61(5):505-9.
24. Jerome Friedman TH, Robert Tibshirani. Regularization Paths for Generalized Linear Models via Coordinate Descent. *Journal of Statistical Software*, 33(1), 1-22. 2010.
25. Zhan X, Hu Y, Li B, Abecasis GR, Liu DJ. RVTESTS: an efficient and comprehensive tool for rare variant association analysis using sequence data. *Bioinformatics*. 2016;32(9):1423-6.
26. The statistical evaluation of medical tests for classification and prediction. [press release]. Oxford, UK: Oxford University Press 2003.
27. Strobl C, Boulesteix AL, Zeileis A, Hothorn T. Bias in random forest variable importance measures: illustrations, sources and a solution. *BMC Bioinformatics*. 2007;8:25.
28. Team RCR. A Language and Environment for Statistical Computing. 2013.
29. Max Kuhn. Contributions from Jed Wing SW, Andre Williams, Chris Keefer, Allan Engelhardt, Tony Cooper, Zachary Mayer, Brenton Kenkel, the R Core Team, Michael Benesty, Reynald Lescarbeau, Andrew Ziem, Luca Scrucca, Yuan Tang and Can Candan. caret: Classification and Regression Training. R package version 6.0-71. 2016.
30. Bedogni G, Bellentani S, Miglioli L, Masutti F, Passalacqua M, Castiglione A, et al. The Fatty Liver Index: a simple and accurate predictor of hepatic steatosis in the general population. *BMC Gastroenterol*. 2006;6:33.
31. Lee JH, Kim D, Kim HJ, Lee CH, Yang JI, Kim W, et al. Hepatic steatosis index: a simple screening tool reflecting nonalcoholic fatty liver disease. *Dig Liver Dis*. 2010;42(7):503-8.



32. Fedchuk L, Nascimbeni F, Pais R, Charlotte F, Housset C, Ratzu V, et al. Performance and limitations of steatosis biomarkers in patients with nonalcoholic fatty liver disease. *Aliment Pharmacol Ther.* 2014;40(10):1209-22.
33. Alberti KG, Zimmet P, Shaw J, Group IDFETFC. The metabolic syndrome--a new worldwide definition. *Lancet.* 2005;366(9491):1059-62.
34. Sudlow C, Gallacher J, Allen N, Beral V, Burton P, Danesh J, et al. UK biobank: an open access resource for identifying the causes of a wide range of complex diseases of middle and old age. *PLoS Med.* 2015;12(3):e1001779.
35. Lean ME, Leslie WS, Barnes AC, Brosnahan N, Thom G, McCombie L, et al. Primary care-led weight management for remission of type 2 diabetes (DiRECT): an open-label, cluster-randomised trial. *Lancet.* 2018;391(10120):541-51.
36. Araujo AR, Rosso N, Bedogni G, Tiribelli C, Bellentani S. Global epidemiology of non-alcoholic fatty liver disease/non-alcoholic steatohepatitis: What we need in the future. *Liver Int.* 2018;38 Suppl 1:47-51.
37. Motamed N, Sohrabi M, Ajdarkosh H, Hemmasi G, Maadi M, Sayeedian FS, et al. Fatty liver index vs waist circumference for predicting non-alcoholic fatty liver disease. *World J Gastroenterol.* 2016;22(10):3023-30.
38. Poynard T, Ratzu V, Naveau S, Thabut D, Charlotte F, Messous D, et al. The diagnostic value of biomarkers (SteatoTest) for the prediction of liver steatosis. *Comp Hepatol.* 2005;4:10.
39. Baranova A, Liotta L, Petricoin E, Younossi ZM. The role of genomics and proteomics: technologies in studying non-alcoholic fatty liver disease. *Clin Liver Dis.* 2007;11(1):209-20, xi.
40. Eslam M, Valenti L, Romeo S. Genetics and epigenetics of NAFLD and NASH: Clinical impact. *J Hepatol.* 2018;68(2):268-79.
41. Wood GC, Chu X, Argyropoulos G, Benotti P, Rolston D, Mirshahi T, et al. A multi-component classifier for nonalcoholic fatty liver disease (NAFLD) based on genomic, proteomic, and phenomic data domains. *Sci Rep.* 2017;7:43238.
42. Eslam M, Hashem AM, Romero-Gomez M, Berg T, Dore GJ, Mangia A, et al. FibroGENE: A gene-based model for staging liver fibrosis. *J Hepatol.* 2016;64(2):390-8.
43. Alonso C, Fernandez-Ramos D, Varela-Rey M, Martinez-Arranz I, Navasa N, Van Liempd SM, et al. Metabolomic Identification of Subtypes of Nonalcoholic Steatohepatitis. *Gastroenterology.* 2017;152(6):1449-61 e7.
44. Danford CJ, Yao ZM, Jiang ZG. Non-alcoholic fatty liver disease: a narrative review of genetics. *J Biomed Res.* 2018;32(5):389-400.
45. Al-Fayoumi S, Hashiguchi T, Shirakata Y, Mascarenhas J, Singer JW. Pilot study of the antifibrotic effects of the multikinase inhibitor pacritinib in a mouse model of liver fibrosis. *J Exp Pharmacol.* 2018;10:9-17.
46. Hagstrom H, Stal P, Hultcrantz R, Brismar K, Ansurudeen I. IGFBP-1 and IGF-I as markers for advanced fibrosis in NAFLD - a pilot study. *Scand J Gastroenterol.* 2017;52(12):1427-34.
47. Petaja EM, Zhou Y, Havana M, Hakkarainen A, Lundbom N, Ihalainen J, et al. Phosphorylated IGFBP-1 as a non-invasive predictor of liver fat in NAFLD. *Sci Rep.* 2016;6:24740.
48. Adamek A, Kasprzak A. Insulin-Like Growth Factor (IGF) System in Liver Diseases. *Int J Mol Sci.* 2018;19(5).

49. Chen Y, Huang H, Xu C, Yu C, Li Y. Long Non-Coding RNA Profiling in a Non-Alcoholic Fatty Liver Disease Rodent Model: New Insight into Pathogenesis. *Int J Mol Sci.* 2017;18(1).
50. Gaggini M, Carli F, Rosso C, Buzzigoli E, Marietti M, Della Latta V, et al. Altered amino acid concentrations in NAFLD: Impact of obesity and insulin resistance. *Hepatology.* 2018;67(1):145-58.
51. Imhasly S, Naegeli H, Baumann S, von Bergen M, Luch A, Jungnickel H, et al. Metabolomic biomarkers correlating with hepatic lipidosis in dairy cows. *BMC Vet Res.* 2014;10:122.
52. Koch M, Freitag-Wolf S, Schlesinger S, Borggrefe J, Hov JR, Jensen MK, et al. Serum metabolomic profiling highlights pathways associated with liver fat content in a general population sample. *Eur J Clin Nutr.* 2017;71(8):995-1001.
53. Uhlen M, Karlsson MJ, Hober A, Svensson AS, Scheffel J, Kotol D, et al. The human secretome. *Sci Signal.* 2019;12(609).
54. Uhlen M, Fagerberg L, Hallstrom BM, Lindskog C, Oksvold P, Mardinoglu A, et al. Proteomics. Tissue-based map of the human proteome. *Science.* 2015;347(6220):1260419.

## **SUPPORTING INFORMATION CAPTIONS**

**S1 Text.** QC of the transcriptomic, proteomic, and metabolomic

**S1 Fig.** Violin plot showing the distribution of liver fat percentage (y-axis) for the diabetic and non-diabetic cohorts (x-axis) of IMI DIRECT.

**S2 Fig.** Distribution of liver fat percentage (y-axis) among the different centers (x-axis) contributing to the IMI DIRECT cohorts.

**S3 Fig.** Manhattan plot showing SNPs associated with liver fat level (~18 million imputed SNPs) in the IMI DIRECT cohorts. The chromosomal position is plotted on the x-axis and the statistical significance of association for each SNP is plotted on the y-axis. Red line indicates genome-wide significance level ( $5 \times 10^{-8}$ ) and the blue line corresponds to the significance level of  $5 \times 10^{-6}$ .

**S4 Fig.** Quantile-quantile (QQ) plot showing results of genome-wide association study (GWAS) for liver fat content in the IMI DIRECT consortium (1514 individuals). X-axis illustrates the expected distribution of *p*-values from association test across all the SNPs and the y-axis shows the observed *p*-values.

**S5 Fig.** Measurements of F1, sensitivity, specificity and balanced accuracy (y-axis) at different cut-offs (x-axis) for model 1 in the diabetic, non-diabetic and the combined cohorts of the IMI-DIRECT.

**S6 Fig.** Measurements of F1, sensitivity, specificity and balanced accuracy (y-axis) at different cut-offs (x-axis) for model 2 in the diabetic, non-diabetic and the combined cohorts of the IMI-DIRECT.

**S7 Fig.** Variable importance for the clinical model (only top 20)

**S8 Fig.** Variable importance for the genetic model (only top 20)

**S9 Fig.** Variable importance for the transcriptomic model (only top 20)

**S10 Fig.** Variable importance for the exploratory proteomic model (only top 20)

**S11 Fig.** Variable importance for the targeted metabolomic model (only top 20)

**S1 Table.** The list of the clinical input variables with the abbreviation used in the analyses and their meaning

**S2 Table.** Characteristics of the study in the non-diabetes, diabetes and combined cohorts separated for participants from IMI DIRECT who had MRI data vs. those who did not have MRI data. Values are median (interquartile range) unless otherwise specified.

**S3 Table.** Variables used to construct each of the NAFLD prediction models developed in the IMI DIRECT.

**S4 Table.** UK Biobank fields used in the analyses.

**S5 Table.** The ROCAUC results of the clinical models in the non-diabetes and diabetes cohorts separately.

**Supporting Information (Excel file).** The details of the LASSO selected features of the omics layers.